Modelling & analysis of the dynamics of pendulum chain

Yuanming Tao
School of Mathematics & Statistics, University of Sydney, NSW 2006, Australia

Modelling of an ideal model of multi-mass pendulum chain. We observed chaos and studied the initial-condition dependent, quasi-periodic motion as time progress, or with different number of masses on the chain. We also analysed kinetic and total energies to find conservation of energy. And studied total and available energies to confirm thermodynamic behaviour in long chains.

I. INTRODUCTION

A common example for chaotic dynamic systems is the pendulum chain. Dynamics in a double-chain pendulum has been explored by Schuster in 1984 as one of the most simple examples of classical chaos. [1] Many variants of the system have been explored, including: horizontally shaken pendulum chain by Alexander, Sidhu & Kevrekidis in 2014 [2], double-square pendulum by Rafat, Wheatland & Bedding in 2016. [3]

In this manuscript, we investigate the dynamics and energies of an idealistic model of multi-mass pendulum chain system, with each masses connect by frictionless hinges & identical inelastic rods. Their movement restricted on a plane. Using animation, trajectory plots, phase portraits and Fourier transforms, we specifically look at the problem where the last mass in the chain is given a force from a still state.

This manuscript is organised as follows: Section II will present a guide to the idealistic mechanical model. Section III presents the standard algorithm constructed, including Runge Kutta method for time-stepping, using *Python*. Section IV is a summary of codes written. Section V is the modelling results and discussions, including efficiency analysis, dynamics analysis and energy analysis.

II. MECHANICAL MODEL

To construct the model of a pendulum chain, we first start from the mechanical balance of force for a single pendulum. Considering it's motion in terms of angular velocity, the balance between tension and gravitational pull

$$m\theta''(t) = -\frac{g}{l}\sin\theta$$

where g is the gravitational constant, m is the mass and θ is the angle between the pendulum rod and the vertical z-axis. The first order derivative of θ is the angular velocity ω. Extrapolating this equation for N-masses with constraints of inelasticity in connection, balance of tension force with gravitational pull Dr. Geoffrey Vasil obtained the model

$$\boldsymbol{L}\cdot\boldsymbol{T} = \boldsymbol{\omega}^2 + \boldsymbol{e}_0\cos\theta_0 \tag{1}$$

where the angular velocity vector,

$$\boldsymbol{\omega} = \frac{d\boldsymbol{\theta}}{dt} \tag{2}$$

and it's derivative, the angular acceleration

$$\frac{d\boldsymbol{\omega}}{dt} = \boldsymbol{D}\cdot\boldsymbol{T} - \boldsymbol{e}_0\sin\theta_0 \tag{3}$$

where $\boldsymbol{T}$ are is a column vector of tensions experienced by the masses. $\boldsymbol{e}_0$ is a column vector with 0's in all entries expect the first, which is a 1. $\boldsymbol{L}(\boldsymbol{\theta})$ & $\boldsymbol{D}(\boldsymbol{\theta})$ are symmetric and anti-symmetric sparce matrices that mimics a first and second-oder finite-difference derivatives respectively. This is a brief summary of an optimised mechanical model of the pendulum chain, formulated by Dr. Geoffrey Vasil in 2018.

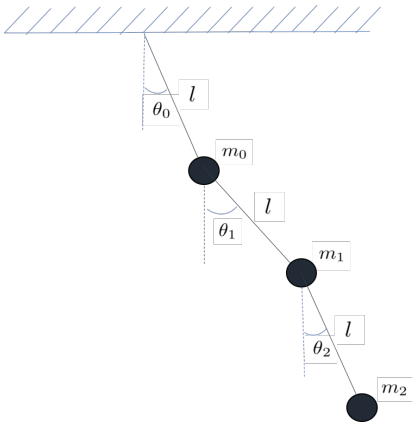

FIG. 1. Basic schematic of a 3 mass pendulum chain

Figure 1 is an simple pendulum chain system with 3 masses. Considering local angles, we can summarise the Cartesian coordinate of the masses in the chain to be a sum of sine or cosine of angle distribution, *i.e.*

$$x_k = \sum_{i=1}^{k-1}\sin\theta_i \quad \text{and} \quad z_k = \sum_{i=1}^{k-1} -\cos\theta_i$$

and their velocities

$$v_{x_k} = \sum_{i=0}^{k-1}\omega_i\cos\theta_i \quad \text{and} \quad v_{z_k} = \sum_{i=0}^{k-1}\omega_i\sin\theta_i$$

III. ALOGIRTHM

For an inital state, we define an initial state vector as the concatenation of the angles and angular velocities vectors.

$$\boldsymbol{l} = \begin{pmatrix} \boldsymbol{\theta} \\ \boldsymbol{\omega} \end{pmatrix}$$

we define the mechanical system as a function $\boldsymbol{f}$, such that

$$\frac{d\boldsymbol{l}}{dt} = \boldsymbol{f}(\boldsymbol{l}) \tag{4}$$

To solve the function, we first unpack $\boldsymbol{l}$ into the angles and angular velocity vector components,

$$\begin{aligned} \boldsymbol{\theta} &= \boldsymbol{l}_i \quad \text{for} \quad 0 \leq i \leq N-1 \\ \boldsymbol{\omega} &= \boldsymbol{l}_j \quad \text{for} \quad N \leq j \leq 2N \end{aligned}$$

Then we compute the difference between angles $\boldsymbol{\delta}$, where

$$\delta_j = \theta_{k+1} - \theta_k \quad \text{for} \quad 0 \leq k \leq N-2$$

And construct banded matrices $\boldsymbol{L}(\boldsymbol{\delta})$ and $\boldsymbol{D}(\boldsymbol{\delta})$,

$$\boldsymbol{D}(\boldsymbol{\delta}) = \begin{pmatrix} 0 & \sin\delta_0 & 0 & 0 & 0 \\ -\sin\delta_0 & 0 & \sin\delta_1 & 0 & 0 \\ 0 & -\sin\delta_1 & 0 & \ddots & 0 \\ 0 & 0 & \ddots & 0 & \sin\delta_{N-2} \\ 0 & 0 & 0 & -\sin\delta_{N-2} & 0 \end{pmatrix}$$

$$\boldsymbol{L}(\boldsymbol{\delta}) = \begin{pmatrix} 1 & \cos\delta_0 & 0 & 0 & 0 \\ \cos\delta_0 & 2 & \cos\delta_1 & 0 & 0 \\ 0 & \cos\delta_1 & 2 & \ddots & 0 \\ 0 & 0 & \ddots & 2 & \cos\delta_{N-2} \\ 0 & 0 & 0 & \cos\delta_{N-2} & 2 \end{pmatrix}$$

The we compute of right hand side of equation (1),

$$\boldsymbol{R} = \boldsymbol{\omega}^2 + \boldsymbol{e}_0 \cos\theta_0$$

where the quadratic term of angular velocity, $\boldsymbol{\omega}^2$, indicates element by element multiplication and $\boldsymbol{R} = \boldsymbol{L} \cdot \boldsymbol{T}$. Then we can invert the matrix to solve for the tension vector. Using the tension vector we can compute the right hand side of equation (3),

$$\boldsymbol{\alpha} = \boldsymbol{D} \cdot \boldsymbol{T} - \boldsymbol{e}_0 \sin\theta_0$$

Then the output of the function is the concatenation of the angular velocities vector and the vector $\boldsymbol{\alpha} = \frac{d\boldsymbol{\omega}}{dt}$,

$$\boldsymbol{f}(\boldsymbol{l}) = \begin{pmatrix} \boldsymbol{\omega} \\ \boldsymbol{\alpha} \end{pmatrix}$$

This was formulated in *Python* as class `chain` of script `pendulum.py`. [**?**]

Using Runge Kutta methods we can solve the derivative in equation (4),

$$l_{n+1} = l_n + h \sum_{m=1}^{s} b_m k_m$$

where

$$\begin{aligned} k_1 &= f(l_n) \\ k_2 &= f(l_n + h(a_{21}k_1)) \\ k_3 &= f(l_n + h(a_{31}k_1 + a_{32}k_2)) \\ &... \\ k_m &= f\left(l_n + h\sum_{j=1}^{m-1} a_{mj}k_j\right) \end{aligned}$$

Tableus of a and b that we can implement includes Fehlberg, Cash-Karp and Dormand-Prince. [4] These methods is formulated in *Python* as class `timestepper` of script `pendulum.py`.

IV. CODE SUMMARY

All code for this project is included in the script `pendulum.py`. Main components of this script includes two classes, `chain` and `timestepper`, and functions for convenient modelling and analysis.

Class `chain` includes: an standard algorithm for the mechanical model, an alternative code for the same algorithm `alt_f`, function `coordinates` to determine the cartesian coordinates of each mass, function `perturb_fstill` to create initial state of all massess still with only the last mass with perturbation of non-zero angular velocity $\omega_N \neq 0$. This class also includes functions `velocities`, `kpe`, `total_energy`, `available_energy` to calculate physical properties of the system corresponding to their names. Note that function `kpe` calculates the kinetic and potential energy for the entire chain or for individual masses.

Class `timestepper` is the python formulation of the Runge-Kutta method, with selection different methods through importing tableau from script `rk_base.py` and calculation of step-size after each step.

Functions `solve` and `dynamics` that implements the two classes and functions for convenience in modelling, the latter includes calculation of energies. Functions `animate` and `animate_path` animates the motion of the pendulum chain, while function `path` shows the path of an individual mass and function `phasep` plots the phase portrait.

Functions `plotter` and `indi_anal` calculates and plots the Fourier transform, power spectrum and log-log power spectrum of calculated energies.

V. RESULTS AND DISCUSSION

A. Efficiency analysis

The code was tested for $N = 1000, 2000, 5000$, with corresponding initial perturbations of $\omega_0 = 50, 100, 250$. According to results in Table 1, calculations of energies is not computational expensive. For increasing number of masses and proportional increase of perturbation, time requirement increase linearly while peaking around $N = 1200$.

N	ω_0	Mean (s)	STD (s)	Mean* (s)	STD* (s)
1000	50	17	0.91	18.2	1.18
2000	100	24.1	2.47	22.6	1.87
5000	250	39	2.37	37.4	1.89

Table 1. Results of `timeit` for time range $T = 200$, initial step-size of $dt = 0.01$ and data collection frequency of every 20 steps. Mean* and STD* are results of implementing the helper funtion `solve` while Mean* and STD* are results of function `dynamics` which includes calculation of energies.

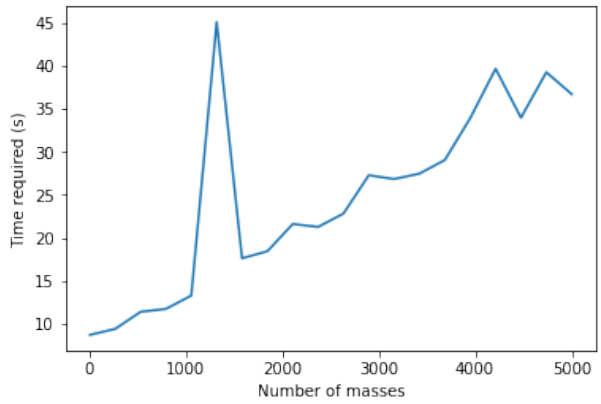

FIG. 2. Efficiency testing for 10 to 5000 masses with increasing initial perturbation 1/20 of number of masses, time range $T = 200$, initial step-size of $dt = 0.01$ and data collection frequency of every 20 steps

The most time consuming component of the code is the `solve_banded` function from `scipy.sparse.linalg` used to solve for the tension vector. Note that that setting of initial perturbation too high will cause overflow due to insufficiency in storage precision. We set ω in our code to be of type `double` to increase the overflow limit. A safe approx. maximum ω_0 is around a quarter of the number of masses N.

B. Chaos in the motion of the pendulum chain

Schuster in 1984 found the simplest example of chaos to be the motion of a double-chain pendulum. We confirm this through modelling a two mass pendulum chain. Plotting the path of the motions of the two masses for perturbation of $\omega_N = 1$ from an initially still hanging state, we can see that the path is much wider for the 2-nd mass, but no obvious chaos is presented. If we increase the perturbation to $\omega_N = 3$, then as we can see from Figure 3, the paths becomes chaotic.

Through phase plots in Figure 4, we can clearly observe uniformity for chain with perturbation of $\omega_N = 1$, where the path of the second mass encloses path of first mass, while displaying high similarity with more periods. The multi-period behaviour in the both masses is a sign of the system approaching chaotic behaviour. [5] If we increase the perturbation to $\omega_N = 3$, then the periodic behaviour is reduced, paths covers a large part of the phase plot, indicating chaos in the motion of the pendulum chain.

To further validate chaos, in Figure 5 we slightly changed the perturbation to $\omega_N = 2.9$ and $\omega_N = 3.2$, comparing the trajectories of second masses to the trajectory of $\omega_N = 3$ perturbated chain in Figure 3, we see significant changes, which indicates high sensitivity of the system on initial conditions. This dependency on initial conditions is the key feature of chaos.

C. Analysis of dynamics

Pendulum chains with enough masses and large enough perturbation displays bouncing motions whist the chain is perfectly in-extendable. A likely explanation is the large degrees of freedom present in the chain. This kind of motions can be seen in trajectories of masses at the end of chain in Figure 6. As the number of masses increases, the frequency of bouncing motion is reduced, while the chain displays a wave-like behaviour.

Motion of pendulum chains tends to be less chaotic with increasing number of masses. In Figure 6, we also plotted the phase portraits of the end masses for a number of chains with $N = 10$ to $N = 1000$. One feature of the plot is the merger of two cycles into one. In Figure 7, we attempt to explore this through modelling chains with mass number between $N = 10$ and $N = 50$, where it's discovered that the the merged cycles separates and recombines frequently before reaching the final combined cycle. Centres of cycles are around 0, 6 and 12, corresponding to approximately 0, 360 and 720 degrees, indicating it's origin been 'full circle' trajectories. For $N > 50$, separation no longer occurs, since as number of masses increases, initial perturbation will become insufficient for this kind of motion, thus reaching a cycle in the phase portrait.

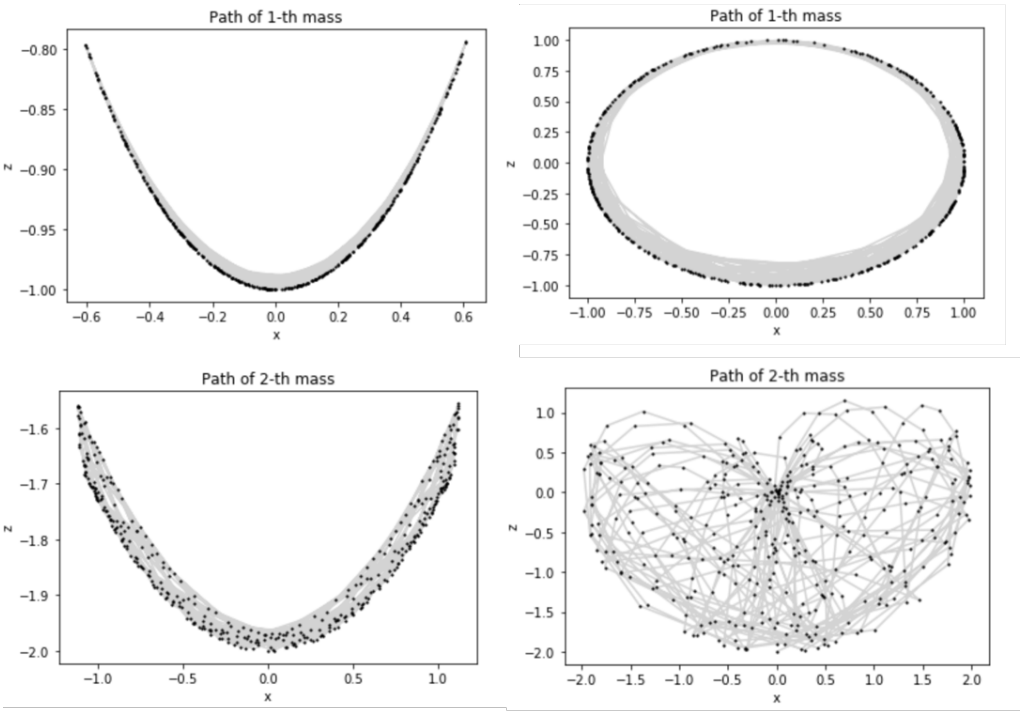

FIG. 3. Modelling of a double chain pendulum. Plots on the left are paths of the motion of individual masses for initial perturbation of $\omega_N = 1$ while plots on the right are for $\omega_N = 3$

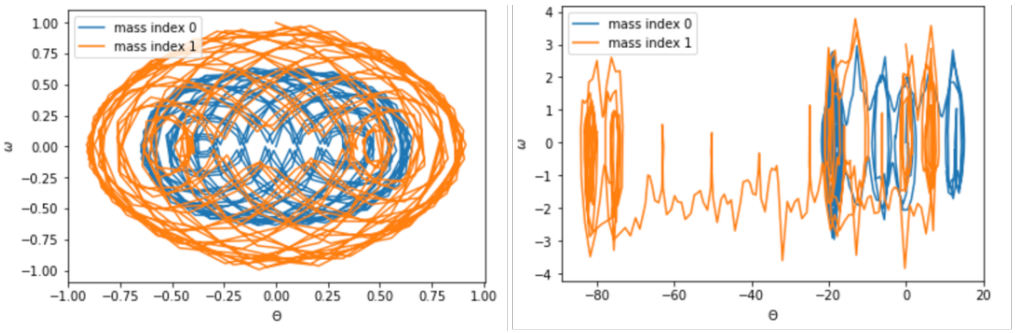

FIG. 4. Modelling of a double chain pendulum. Phase portraits for initial perturbation of $\omega_N = 1$ while plots on the right are for $\omega_N = 3$. Individual masses are plotted in different colors.

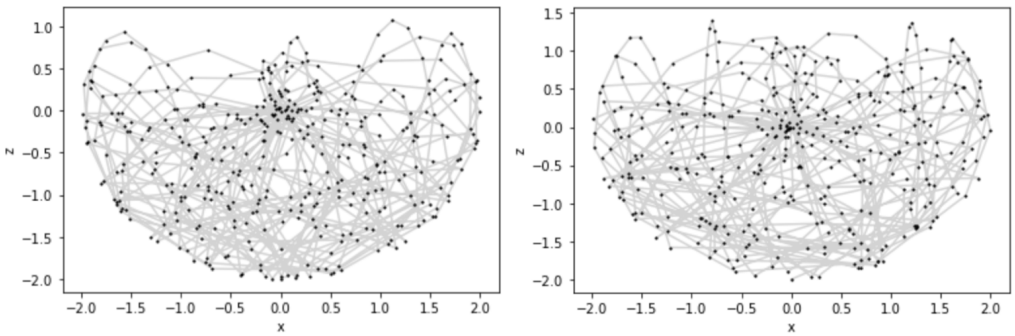

FIG. 5. Modelling of a double chain pendulum. Paths of the second mass for initial perturbation of $\omega_N = 2.9$ (left) and $\omega_N = 3.2$ (right).

Reduction of path spread in the phase portrait indicates reducing chaos with higher number of masses.

For further validation, we plot phase portraits for the tenth mass and the first mass on the pendulum chain in Figure 8. As the number of masses increases, paths of the tenth mass tends towards the first mass. So the motion of individual masses becomes 'synchronised' with masses closer to the origin. Converging phase portraits indicates reduction in randomness in motion of the higher masses, resulting in reduction in initial condition sensitivity, thus less chaotic behaviour. Note that the double periodic behaviour still exists for all $N > 10$, so motion of the chain still approached chaos.

D. Analysis of total & available energies

Total energy of the pendulum chain, consisting of kinetic and potential energy components, is

$$E = \underbrace{\frac{1}{2}\sum_{k=1}^{N} v_{x_k}^2 + v_{z_k}^2}_{KE} + \underbrace{\sum_{k=1}^{N} z_k}_{PE}$$

while the available energy,

$$A = \frac{1}{2}\sum_{k=0}^{N-1}\left(v_{x_k}^2 + v_{z_k}^2 - 4(N-k)\cos^2\left(\frac{\theta_k/2}{2}\right)\right)$$

In Figure 9, we plotted the available and total energies for pendulum chains of various length. For chains with only a small number of masses, there exists a fixed difference between total & available energies (in this case for $N = 10$, $\omega_N = 50$, difference is a fixed value of 55 J). For chains with large number of masses, this difference is no longer fixed and the available energies becomes the inversion of total energies with respect to a mean difference between them.

Reduction of available energy indicates 'thermodynamic' behaviour in the long pendulum chains. Available energy is transformed into unavailable energy as it reduces. This is an entropy increasing process due to the second law of thermodynamics, which states that total entropy does not decrease with time. Since entropy is the possible energy distributions of the system, lower available energy is a trend towards greater disorder. This indicates that for pendulum chains with enough masses (i.e. enough degrees of freedom) the motion becomes more chaotic as time progresses.

D. Analysis of kinetic & potential energies of pendulum chain

In Figure 10, we plotted the overall change in kinetic & potential energies with time and their corresponding power spectrums for chains with various number of masses. Since the same initial perturbation is used for these chains, frequency 'beats' which relates to changes in kinetic or potential energies reduces as the number of masses increases.

Notice that while change in amplitude is the same for kinetic and potential energies, potential energy deviates significantly from 0 as compared to kinetic energy. This is due to the fact that potential energies, even at maximum kinetic energies, remains non-zero. While kinetic energies approaches 0 when the pendulum chain reaches a relatively high position. A physical explanation for this is that the pendulum, even at the still state, is above ground and so there exists balance between gravitational potential and tension forces at the point of maximum kinetic energy.

Similarity between the power spectrums of kinetic and potential energy indicates conservation of energies. Since real peaks on the spectrum have harmonics, small deviations between the change of kinetic/potential energies might cause accumulated deviations of the harmonics. High similarity between kinetic and potential energies power spectrums indicates similar changes in kinetic and potential energies. As masses gains kinetic energy, they lose potential energy, *visa versa*.

Also, in the power spectrums for chain with 1000 masses, peaks seems to be enclosed by an oscillating envelope. A wild guess for why this spectral envelop occurs is oscillations between masses in the chain.

E. Analysis of kinetic & potential energies of individual masses

The kinetic and potential energies of individual masses on the pendulum chain are

$$KE_k = \frac{1}{2}v_{x_k}^2 + v_{z_k}^2$$
$$PE_k = z_k$$

Individual energies on chains with 10 and 100 masses are presented in Figure 11 and 12 respectively. In both figures, notice that closer to the centre, change in kinetic/potential energies of masses tends to be similar. Whilst as masses approached the end of the chain, change in energy becomes more uniform. Comparing the two figures, we can further confirm the reduction in kinetic/potential energy frequency of change as number of masses in the chain increases.

Theses plots provides rich amount of interesting features, including similarity in power spectrum peak locations in high frequency regions for 100 mass chain, and similarity in low frequency regions for 10 mass chain. Also, the step like reduction in peaks' amplitudes for

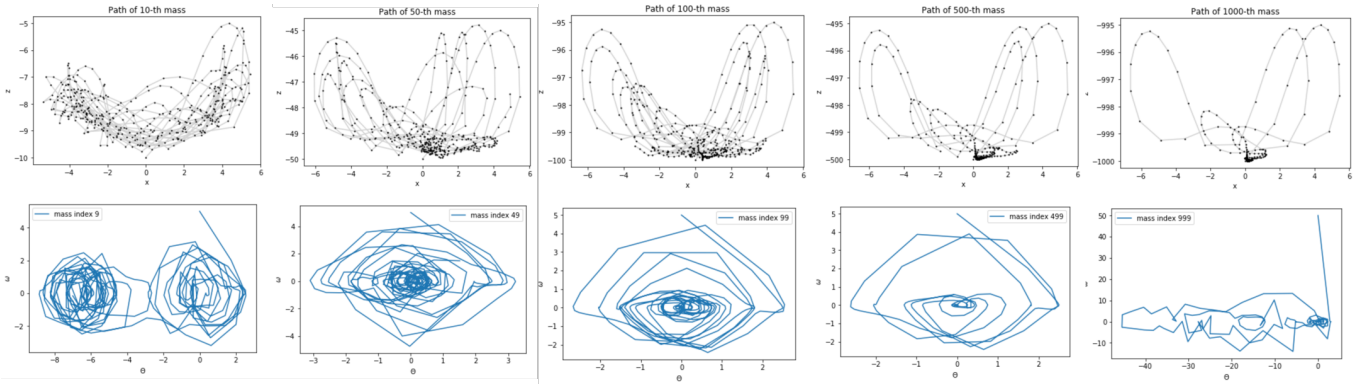

FIG. 6. Modelling of chain pendulum with different number of masses. Top plots presents paths of the last masses, bottom are phase portraits of the last masses. $N = 10, 50, 100, 500, 1000$ for plots from left to right

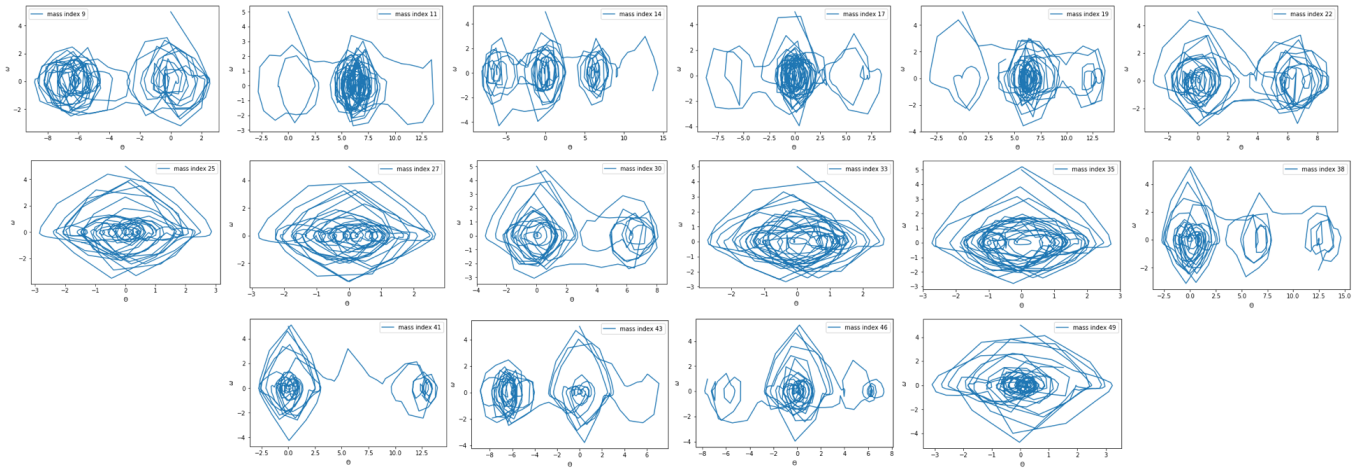

FIG. 7. Modelling of chain pendulum with different number of masses. Phase portraits of the 1st and 10th masses. $N = 10, 20, 30, 40, 50$ for plots from left to right

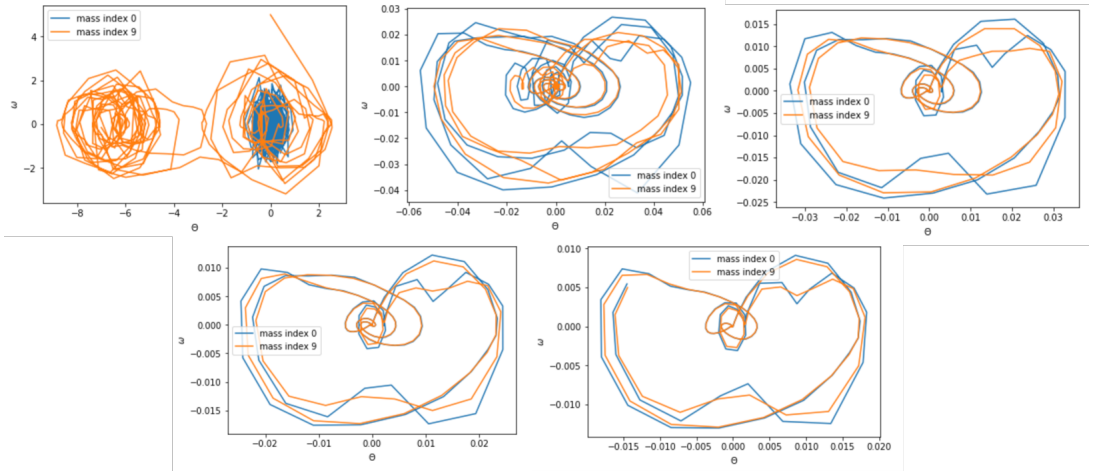

FIG. 8. Modelling of chain pendulum with different number of masses. Phase portraits of the 1st and 10th masses. $N = 10, 230, 450, 670, 1000$ for plots from left to right

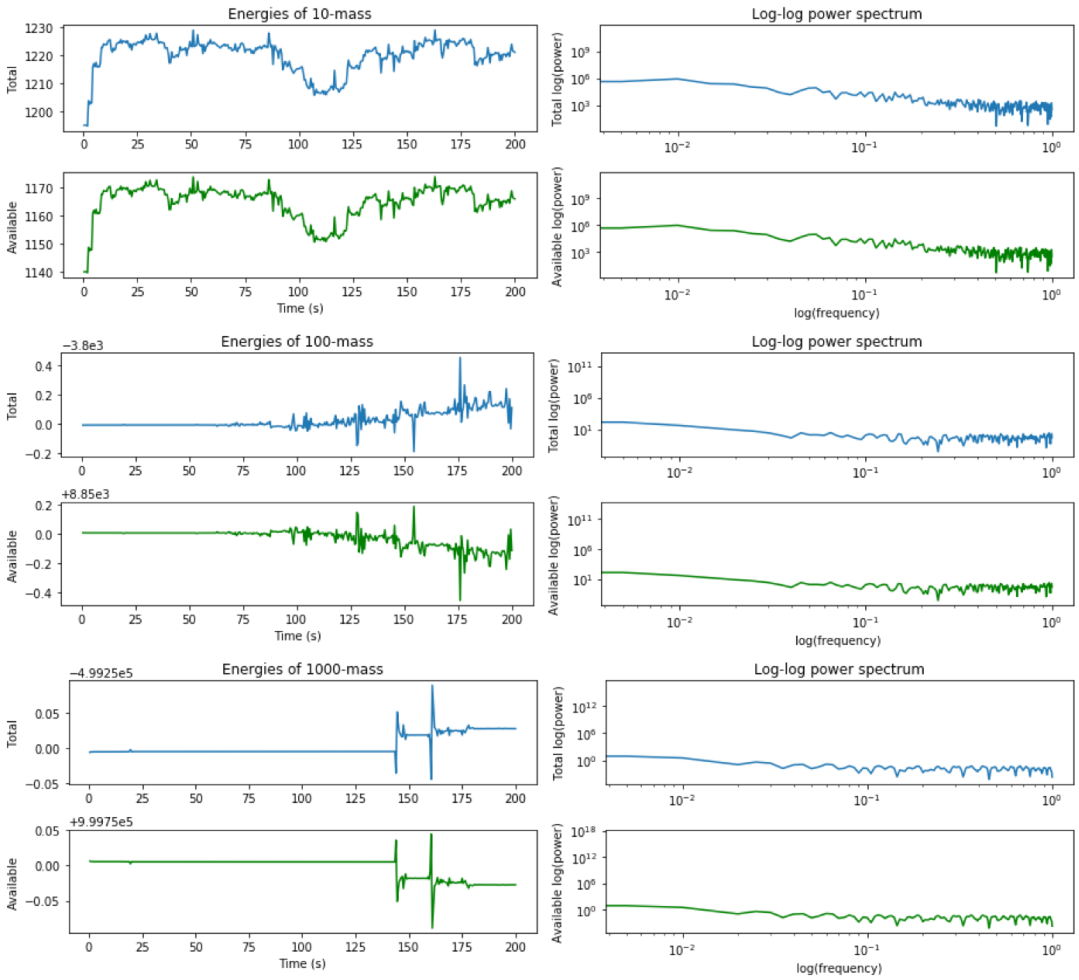

FIG. 9. Energy distribution of chain pendulum with different number of masses. Plot of total & available energies of pendulum chains with mass numbers $N = 10, 100, 1000$ (initial perturbation $\omega_N = 50$ and their corresponding power spectrums in log-log space.

masses close to the origin on the 100 mass chain. Further exploring these features may provide insights into dynamics of chaotic systems.

VI. CONCLUSION

Through modelling of an ideal pendulum chain, we observed chaos in motion of a simple 2-mass chain and verified it's dependence on initial conditions. We observed bouncing motion through animation and analysed the dynamics of multi-mass chains, where the chaotic behaviour reduces as the number of masses on the chain increases. Analysis of available energies showed thermodynamic behaviour inside long chains and indicates increasing chaos as time progresses. Analysis of kinetic and potential energies of the overall chain or individual masses showed conservation and provided a rich amount of spectral feature which be of interest for further investigation. Further studies can include analysis of Poincare sections, the use of low-pass or high-pass filter to investigate spectra and the addition of forces from the environment, e.g. wind, to this ideal model.

ACKNOWLEDGEMENT

The pendulum chain model, equations and efficient code structure are the work of Dr Geoffrey Vasil. Sections of the analysis codes are produced in collaboration with Yuanming Tao, the major contributor. This manuscript is in the compact form of Phys. Rev. AIP template.

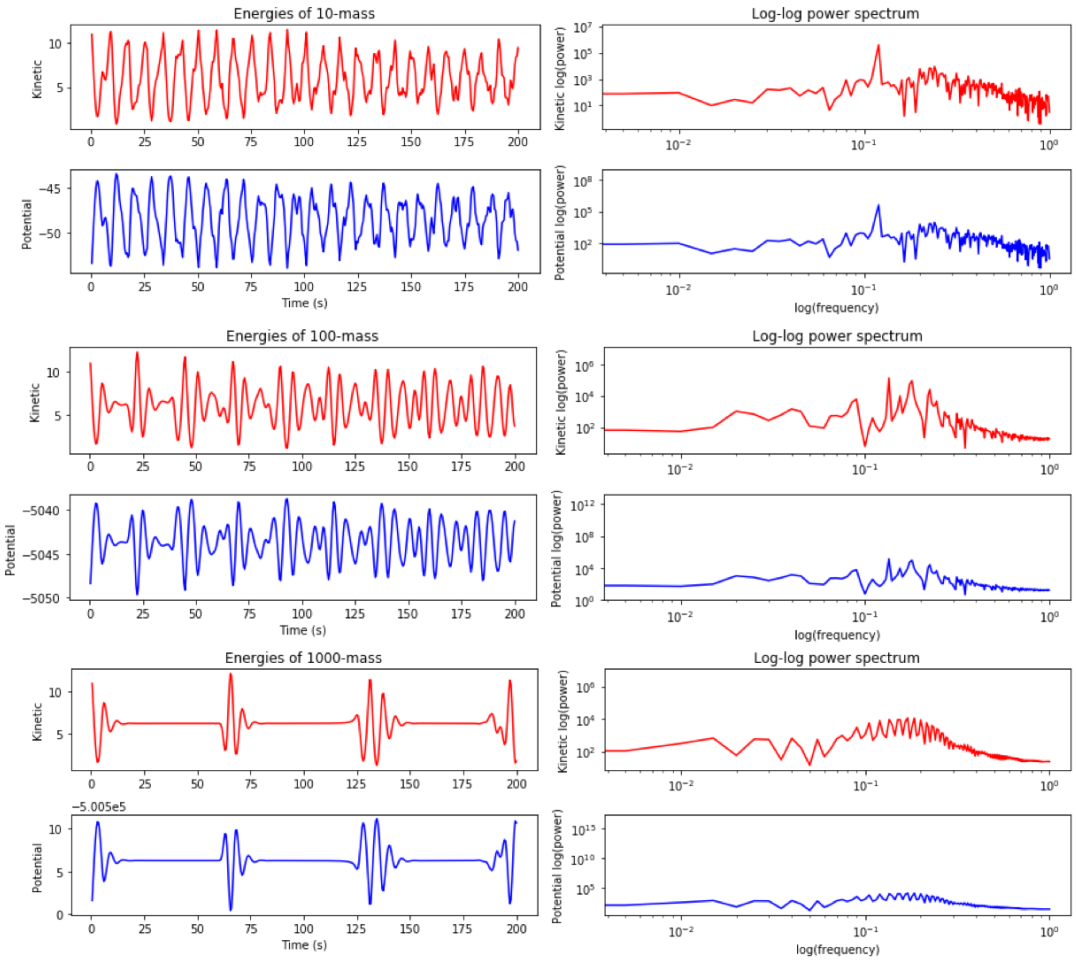

FIG. 10. Kinetic and potential energies on a chain pendulum with $N = 10, 100, 1000$ masses (initial perturbation $\omega_N = 5$) and their corresponding power spectrums in log-log space.

REFERENCES

[1] P. H. Richter and H.J. Scholz, "Chaos in classical mechanics: The double pendulum," in Stochastic Phenomena and Chaotic Behavior in Complex Systems, edited by P. Schuster Springer, Berlin, Heidelberg, 1984", pp. 86-97.

[2] Y. Xu, T. J. Alexander, H. Sidhu, and P. G. Kevrekidis, "Instability dynamics and breather formation in a horizontally shaken pendulum chain". arXiv:1409.6379

[3] M.Z. Rafat, M.S. Wheatland & T.R. Bedding, "Dynamics of a double pendulum with distributed mass". DOI: 10.1119/1.3052072

[4] Wikiwand: List of Runge-Kutta methods, website `www.wikiwand.com/en/List_of_Runge?Kutta_methods`

[5] PHYS1901 Lecture Notes: A Brief Introduction to Chaos Theory

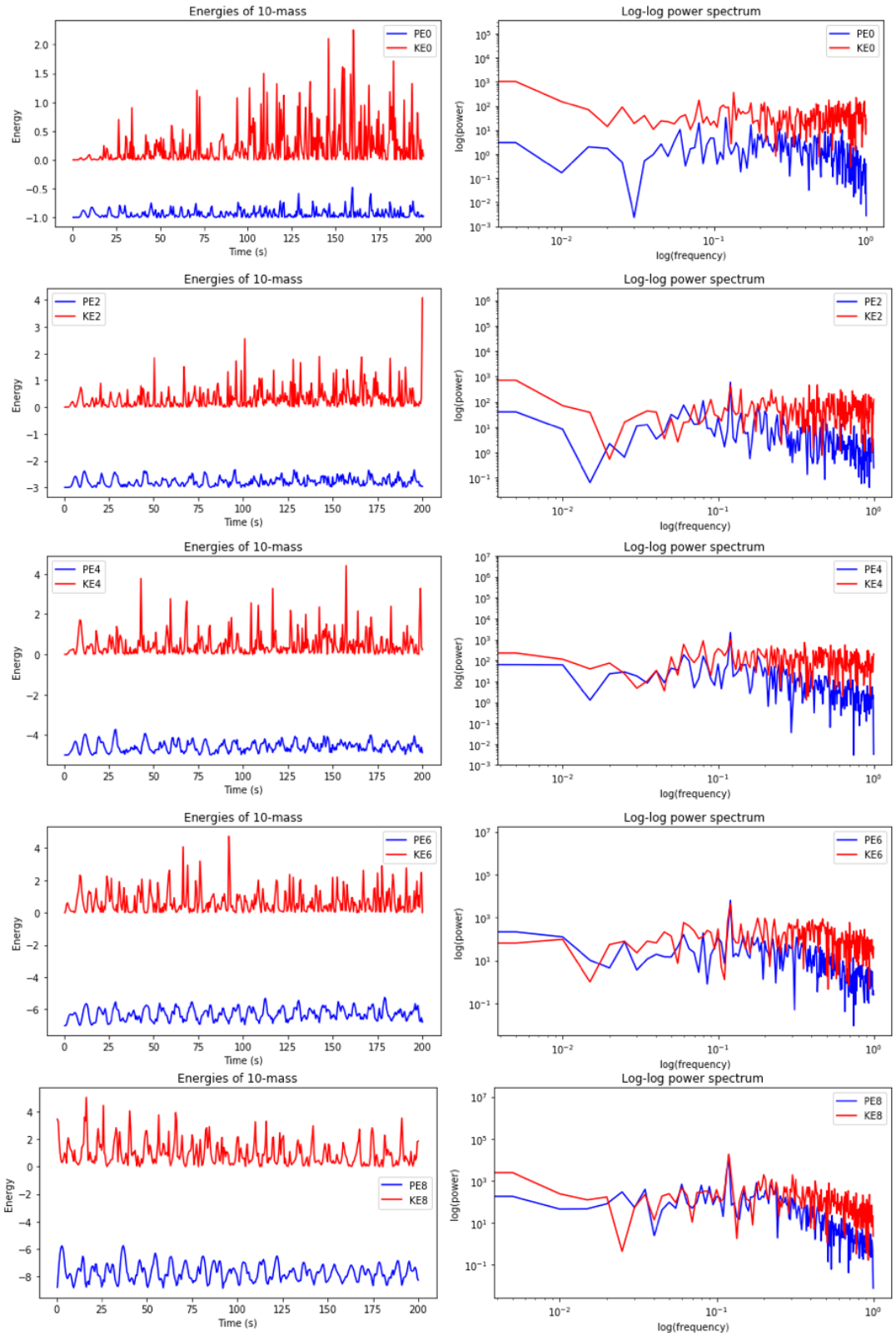

FIG. 11. Kinetic and potential energies on a chain pendulum with $N = 10$ masses (initial perturbation $\omega_N = 5$) and their corresponding power spectrums in log-log space. Index of individual masses chosen are $0, 2, 4, 6, 8$.

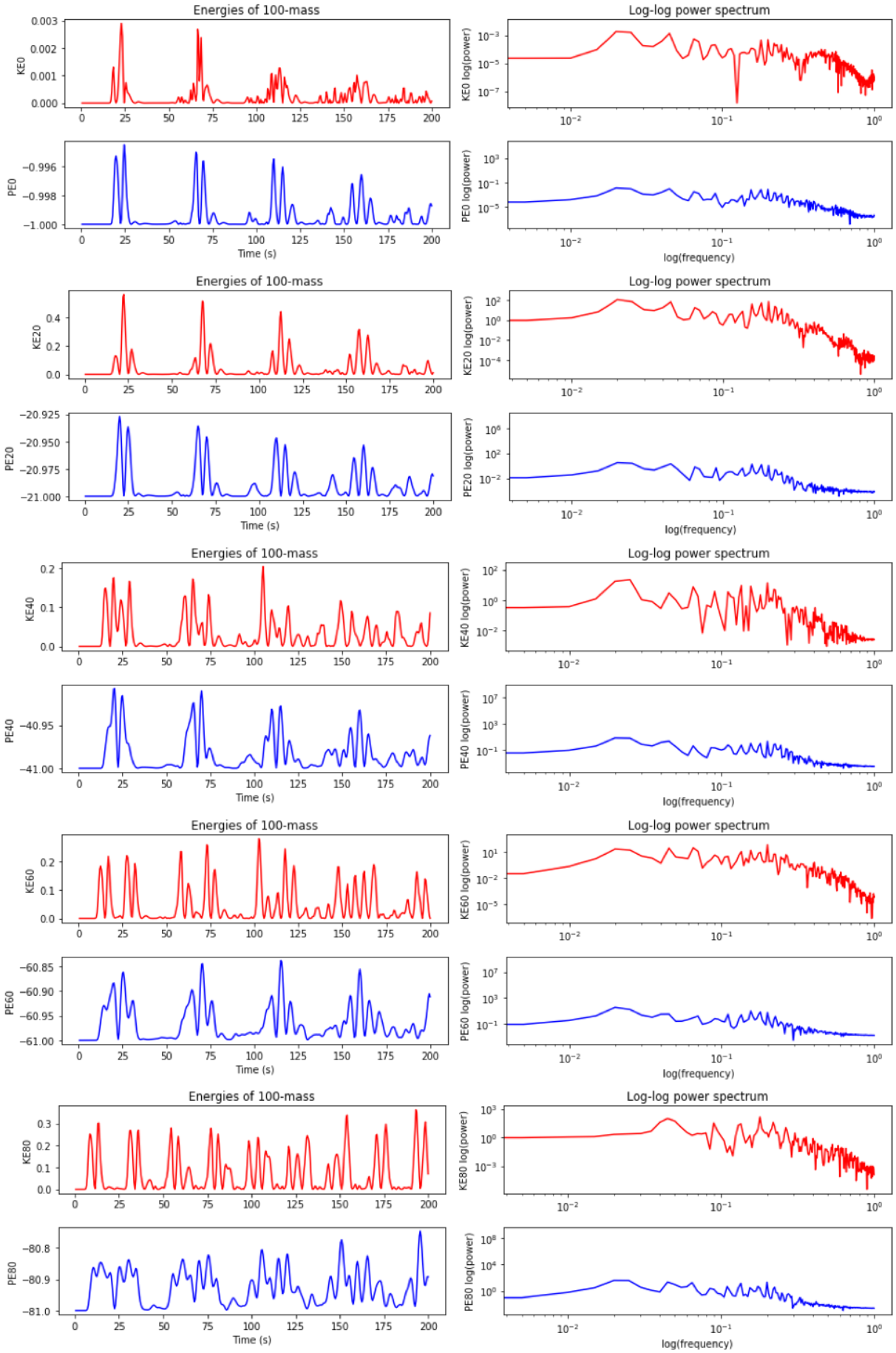

FIG. 12. Kinetic and potential energies of individual masses on a chain pendulum with $N = 100$ masses (initial perturbation $\omega_N = 5$) and their corresponding power spectrums in log-log space.Index of individual masses chosen are $0, 20, 40, 60, 80$.